Physiol. (London) **305**, 279 (1980); B. E. Alger and R. A. Nicoll, *ibid.* **328**, 125 (1982).
49. N. R. Newberry and R. A. Nicoll, *ibid.* **360**, 161 (1985).
50. T. J. Blaxter and G. A. Cottrell, *Quart. J. Exper. Physiol.* **70**, 75 (1985); M. Inoue, T. Matsuo, N. Ogata, *Brit. J. Pharmacol.* **86**, 515 (1985).
51. U. Misgeld, R. A. Deisz, H. U. Dodt, H. D. Lux, *Science* **232**, 1413 (1986).
52. B. H. Gahwiler and D. A. Brown, *Proc. Natl. Acad. Sci. U.S.A.* **82**, 1558 (1985); M. Inoue, T. Matsuo, N. Ogata, *Brit. J. Pharmacol.* **84**, 833 (1985).
53. P. Dutar and R. A. Nicoll, *Nature* **332**, 156 (1988).
54. B. E. Alger and R. A. Nicoll, *J. Physiol. (London)* **328**, 105 (1982).
55. R. A. Nicoll and B. E. Alger, *Science* **212**, 957 (1981); B. E. Alger, *J. Neurophysiol.* **52**, 892 (1984); N. R. Newberry and R. A. Nicoll, *J. Physiol. (London)* **348**, 239 (1984); J. J. Hablitz and R. H. Thalmann, *J. Neurophysiol.* **58**, 160 (1987).
56. D. I. B. Kerr, J. Ong, R. H. Prager, B. D. Gynther, D. R. Curtis, *Brain Res.* **405**, 150 (1987).
57. H. Hasuo and J. P. Gallagher, *Neurosci. Lett.* **86**, 77 (1988); I. Soltesz, M. Haby, N. Leresche, V. Crunelli, *Brain Res.* **448**, 351 (1988); G. Karlsson, M. Pozza, H.-R. Olpe, *Eur. J. Pharmacol.* **148**, 485 (1988).
58. R. Y. Moore and A. E. Halaris, *J. Comp. Neurol.* **164**, 171 (1975).
59. H. Jahnsen, *Brain Res.* **197**, 83 (1980); M. Segal, *J. Physiol. (London)* **303**, 423 (1980).
60. R. Andrade, R. C. Malenka, R. A. Nicoll, *Science* **234**, 1261 (1986).
61. R. Andrade and R. A. Nicoll, unpublished observation.
62. L. O. Trussell and M. B. Jackson, *J. Neurosci.* **7**, 3306 (1987); J. L. Yakel, L. O. Trussell, M. B. Jackson, *ibid.* **8**, 1273 (1988).
63. R. Andrade and G. K. Aghajanian, *ibid.* **5**, 2359 (1985); R. A. North and J. T. Williams, *J. Physiol. (London)* **364**, 265 (1985).
64. M. G. Lacey, N. B. Mercuri, R. A. North, *J. Physiol. (London)*, in press.
65. P. J. Pfaffinger, J. M. Martin, D. O. Hunter, N. M. Nathanson, B. Hille, *Nature* **317**, 536 (1985); G. Breitwieser and G. Szabo, *ibid.* **317**, 538 (1985); D. E. Logothetis, Y. Kurachi, J. Golper, E. J. Neer, D. E. Chaphan, *ibid.* **325**, 321 (1987); A. Yatani, J. Codina, A. M. Brown, L. Birnbaumer, *Science* **235**, 207 (1987).
66. D. Piomelli *et al.*, *Nature* **328**, 38 (1987).
67. P. F. Worley, J. M. Baraban, M. McCarren, S. H. Snyder, B. E. Alger, *Proc. Natl. Acad. Sci. U.S.A.* **84**, 3467 (1987).
68. K. H. Jakobs, S. Bauer, Y. Watanabe, *Eur. J. Biochem.* **151**, 425 (1985).
69. R. Andrade and R. A. Nicoll, *J. Physiol. (London)* **394**, 99 (1987); A. Colino and J. V. Halliwell, *Nature* **328**, 73 (1987).
70. J. D. Wood and C. J. Mayer, *J. Neurophysiol.* **42**, 582 (1979); G. M. Mawe, T. A. Brancheck, M. D. Gershon, *Proc. Natl. Acad. Sci. U.S.A.* **83**, 9799 (1986); A. Suprenant and J. Crist, *Neuroscience* **24**, 283 (1988).
71. C. P. VanderMaelen and G. K. Aghajanian, *Brain Res.* **239**, 139 (1980); P. A. M. Van Dongen, S. Grillner, T. Hökfelt, *ibid.* **366**, 320 (1986).
72. I am greatly indebted to the many individuals with whom I have had the opportunity to work. I thank R. Malenka, J. Kauer, and D. Nicoll for their comments on the manuscript. Research in my lab is supported by NIH grants MH 38256, MH 0437 (RSDA), and NS 24205.

Research Articles

Parallel Stranded DNA

JOHAN H. VAN DE SANDE, NIELS B. RAMSING, MARKUS W. GERMANN, WIM ELHORST, BERND W. KALISCH, EBERHARD V. KITZING, RICHARD T. PON, ROBERT C. CLEGG, THOMAS M. JOVIN

A series of four hairpin deoxyoligonucleotides was synthesized with a four-nucleotide central loop (either C or G) flanked by the complementary sequences $d(T)_{10}$ and $d(A)_{10}$. Two of the molecules contain either a 3′-p-3′ or 5′-p-5′ linkage in the loop, so that the strands in the stem have the same, that is, parallel (ps) polarity. The pair of reference oligonucleotides have normal phosphodiester linkages throughout and antiparallel (aps) stem regions. All the molecules adopt a duplex helical structure in that (i) the electrophoretic mobilities in polyacrylamide gels of the ps and aps oligomers are similar. (ii) The ps hairpins are substrates for T4 polynucleotide kinase, T4 DNA ligase, and *Escherichia coli* exonuclease III. (iii) Salt-dependent thermal transitions are observed for all hairpins, but the ps molecules denature 10°C lower than the corresponding aps oligomers. (iv) The ultraviolet absorption and circular dichroism spectra are indicative of a base-paired duplex in the stems of the ps hairpins but differ systematically from those of the aps counterparts. (v) The bis-benzimidazole drug Hoechst-33258, which binds in the minor groove of B-DNA, exhibits very little fluorescence in the presence of the ps hairpins but a normal, enhanced emission with the aps oligonucleotides. In contrast, the intercalator ethidium bromide forms a strongly fluorescent complex with all hairpins, the intensity of which is even higher for the ps species. (vi) The pattern of chemical methylation is the same for both the ps and aps hairpins. The combined results are consistent with the prediction from force field analysis of a parallel stranded right-handed helical form of $d(A)_n \cdot d(T)_n$ with a secondary structure involving reverse Watson-Crick base pairs and a stability not significantly different from that of the B-DNA double helix. Models of the various hairpins optimized with force field calculations are described.

THE POLYMORPHIC NATURE OF DOUBLE-STRANDED DNA IS well established (*1*, *2*). A common feature of the three major families of A-, B-, and Z-DNA duplexes is the antiparallel disposition of the constituent strands (*2*, *3*). Single crystal diffraction analysis of oligonucleotide duplexes indicates that only Watson-Crick base pairing occurs in the structures examined to date (*3*). However, alternative conformations are feasible. Thus, both experimental evidence and model calculations support the existence of parallel stranded double helices stabilized by (i) hemiprotonation of

J. H. van de Sande, M. W. Germann, B. W. Kalisch, and R. T. Pon are at the Department of Medical Biochemistry, University of Calgary, Calgary, Alberta, Canada T2N 4N1. N. B. Ramsing, W. Elhorst, E. v. Kitzing, R. C. Clegg, and T. M. Jovin are at the Department of Molecular Biology, Max Planck Institute for Biophysical Chemistry, 3400 Göttingen, Federal Republic of Germany.

C, as in the CpA-proflavin complex (*4*), and d(C-T)$_3$ (*5*); (ii) protonation of poly(A) (*6*); and (iii) introduction of bulky substituents (x = dimethylamino, methyl, methylthio) in poly(x^{2}A)·poly(U) (*7*). Triple helices have also been proposed in which two of the strands are demonstrated or presumed to be associated in a parallel orientation stabilized by Hoogsteen base-pairing. [Normal Watson-Crick base-pairing is incompatible with parallel stranded duplexes (*2*, figure 6-2)]. These include (i) the products of disproportionation reactions (*2*), such as poly(A)·2 poly(U) and poly[d(T)]·2 poly[d(A)]; (ii) the protonated or methylated forms of poly[d(pyr)]·poly[d(pur)] (*8*); and (iii) complexes of homopyrimidine oligodeoxynucleotides bearing a chemical cleaving function and bound within the major groove of homopyrimidine-homopurine tracts in DNA (*9*). The hexamer d(T)$_6$ containing methylated phosphate triesters (*10*) and the complexes of α-anomeric oligodeoxynucleotides with complementary oligo-[β]-deoxynucleotides (*11*) constitute further examples of parallel duplex structures. All of the above molecular species contain particular chemical features that either deviate from the primary structure of natural RNA and DNA or involve nonphysiological environmental conditions. However, Pattabiraman has reported a force field calculation for the homopolymeric duplex d(A)$_6$·d(T)$_6$, indicating that a parallel right-handed helix with reverse Watson-Crick base pairing could be energetically as favorable as the conventional antiparallel B-DNA (*12*). We have devised experimental strategies for demonstrating such a structure and present here the results.

Chemical structure and synthesis of DNA fragments. In the design of parallel stranded DNA, we exploited the facilitation of intramolecular duplex formation in DNA hairpin structures. Bipolar phosphodiester bonds were introduced in the backbones of partially self-complementary oligonucleotides in order to impose a parallel orientation to the strands comprising the duplex structures in the resultant hairpins. The structures of the four hairpins synthesized with d(A)$_{10}$·d(T)$_{10}$ stem regions, including the two with the built-in reversal of polarity, are as follows.

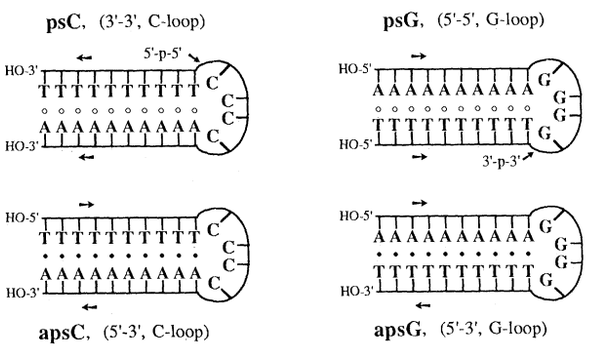

Oligonucleotides psC and psG were designed to have parallel strands with two 3′ termini (achieved with the indicated 5′-p-5′ internucleotide bond) and two 5′ termini (via a 3′-p-3′ bond), respectively. The corresponding control oligonucleotides have the normal 5′-3′ polarity throughout with either 5′-terminal d(T)$_{10}$ and 3′-terminal d(A)$_{10}$ segments (apsC), or the same sequences in reverse order (apsG). Both sets of hairpin structures include loop regions consisting either of dC$_4$ (psC and apsC) or dG$_4$ (psG and apsG).

The polarity reversal in the ps oligonucleotides necessitated some steps of chemical synthesis in the 5′ to 3′ direction, that is, opposite to the conventional 3′-5′ polarity. The preparation of the required phosphoramidite monomer with the cyanoethylphosphoramidite group on the 5′ position is shown in Fig. 1. This orientation of the active groups on the nucleoside allowed for synthesis in the 5′ to 3′ direction during the first ten steps (psG) or the last ten steps (psC). For psG, it was also necessary to prepare a controlled pore glass support with thymidine attached through the 5′-OH group and with the free 3′-OH serving as the growing point. We obtained the hairpin structures with these reagents and protocols and a DNA synthesizer (Applied Biosystems) programmed for the automated phosphoramidite chemistry (*13*). The 24-nucleotide oligomers were purified by high-performance liquid chromatography on a poly(styrene divinylbenzene) resin (PRP-1) (*14*) and by preparative polyacrylamide gel electrophoresis.

Table 1. Thermodynamic parameters for helix-coil transitions of ps and aps hairpins.

Hairpin	T_m* (°C)	ΔH_{vH}† (kJ mol^{-1})	ΔS‡ (J mol^{-1} K^{-1})	ΔG§ (kJ mol^{-1})	Hyperchromicity (%) at 250 nm	267 nm	279 nm
psC	40.2	199	628	12	5	19	18
psG	41.3	192	605	11	4	22	20
apsC	50.8	222	680	19	19	22	7
apsG	51.4	218	670	19	17	22	7

*Melting temperature in 0.1*M* NaCl, 10 m*M* sodium cacodylate, *p*H 7.2. Average values; the results of individual experiments were in the range of ±0.3°C. †van't Hoff melting enthalpy. Average values from determinations in the range of 0.05 to 0.4*M* NaCl; the variations were ±5 percent. ‡Melting entropy in 0.1*M* NaCl, calculated from $\Delta S = \Delta H_{vH}/T_m$. Average values; individual measurements were in the range of ±10 percent. §Free energy difference of transition at 25°C in 0.1*M* NaCl, 10 m*M* sodium acacodylate, *p*H 7.2; calculated from $\Delta G = \Delta H_{vH} - T\Delta S$. Average values; individual measurements were in the range of ±2 percent.

Characterization of ps and aps hairpins by gel electrophoresis and as enzyme substrates. The four oligonucleotides were subjected to polyacrylamide gel electrophoresis under denaturing and native conditions (Fig. 2). In a denaturing urea gel run at 60°C (Fig. 2A), all species show a similar mobility as a marker d(T)$_{24}$ oligomer, although the molecules incorporating a dG$_4$ loop (psG and apsG) migrate at a somewhat slower rate than the corresponding oligomers with a dC$_4$ loop (psC and apsC). These results confirm the total oligonucleotide length and in combination with those gained under native conditions of electrophoresis (Fig. 2B) indicate that the oligomers can adopt duplex hairpin structures. Thus, the two reference antiparallel stranded hairpins apsC and apsG have similar mobilities under native conditions only slightly lower than that of a reference d(A)$_{10}$·d(T)$_{10}$ duplex. The ps oligomers migrate as single bands, well ahead of d(T)$_{24}$, and with psG again slightly trailing psC. There is no evidence for intermolecular antiparallel duplexes in the form of multiple slower moving bands in native gels. The double-stranded nature of all the hairpin structures (aps and ps) is also confirmed by the fluorescence elicited by the bands after staining the gels with the intercalator ethidium bromide (Fig. 2C). However, a contrasting behavior is observed with the A·T specific DNA drug bis-benzimidazole Hoechst-33258 (BBI-258) that binds in the minor groove of B-DNA. The bands corresponding to the aps but not to the ps hairpins are fluorescent after staining with BBI-258 (Fig. 2D). These results are consistent with the solution studies described below.

The hairpins psG, apsG, and apsC were end-labeled with ^{32}P in the presence of T4 polynucleotide kinase (*15*). The psG hairpin in particular is an excellent substrate for the kinase, with both 5′-OH termini serving as acceptors. Upon digestion to 5′ mononucleotides, radioactivity is found in dpA and dpT (1:1) for psG, in dpA for apsG, and in dpT for apsC. As would be expected, no phosphate label can be incorporated into psC because of the absence of 5′-OH acceptor groups. The *Escherichia coli* exonuclease III susceptibility of the ps duplex containing two 3′-OH termini (psC) was also

investigated. Degradation (of both arms) occurs, albeit at a slower rate than that observed with the corresponding control hairpin apsC. The ps hairpins are substrates of T4 DNA ligase. Ligation (at low efficiency) is observed between appropriately phosphorylated linker duplexes and either the parallel stranded duplex with 5′-OH (psG) or 3′-OH (psC) termini. The blunt end ligation allows for the formation of only a single phosphodiester bond in the strand with the normal 5′-3′ alignment. Thus, the enzyme is able to recognize the conventional polarity of the joining site in spite of the presence of the opposite strand in parallel orientation.

Thermodynamic properties of ps and aps hairpins. All hairpins exhibit a thermally induced hyperchromicity at 260 nm, an indication of a cooperative transition from a base-stacked double-stranded structure to a melted random coiled state. Thermal denaturation profiles of the four hairpins were determined by measuring the increase in ultraviolet absorbance upon melting. The data from experiments under various ionic conditions fit well to a concerted, two-state model for the helix-coil transition. The derived (*16*) thermodynamic parameters are summarized in Table 1. The values obtained for the melting temperature (transition midpoint) T_m and the van't Hoff melting enthalpy ΔH_{vH} are independent of the wavelength of analysis and the direction (ascending or descending) of thermal transition. The ΔH_{vH} is also independent of ion concentration, and consistently lower (about 10 percent) for the ps hairpins than for the aps hairpins. The enthalpy change per mole of (nearest neighbor) interaction (*17*), $\Delta h°$, is 22 kJ and 24 kJ for the ps and aps hairpins, respectively, if we assume that the cooperative unit consists of the 10 base pairs in the stem and that the loop makes no significant contribution to the transition enthalpy (*18*). The maximal hyperchromicity of the ps hairpins is as high as that observed for the aps hairpins (Table 1).

The ps hairpins are remarkably stable duplexes, as evidenced by measured T_m values, which are only 10°C lower than those of the corresponding aps reference molecules and show the same pronounced dependence on ionic strength. Thus, $\partial T_m/\partial \log[Na^+]$ is constant in the range 0.05 to 0.4*M* NaCl and the same for all four hairpin species (18° ± 1°), suggesting that the thermodynamic degree of ion dissociation accompanying denaturation is similar (*18*). The constancy of the T_m and ΔH_{vH} values as well as the shape of the transition curves over a sixfold increase in sample concentration constitute evidence that intermolecular dimeric or concatameric structures are not involved.

Optical properties of ps and aps hairpins. The ultraviolet absorption spectra of the ps hairpins at 20°C show distinct differences from those of the corresponding control aps molecules (Fig. 3A). However, the differential contributions from the loops, dC_4

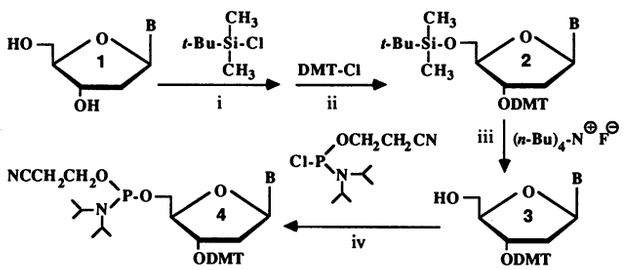

Fig. 1. The synthesis of the 5′phosphoramidite derivative required for the 5′ to 3′ solid-phase synthesis of oligonucleotides. The four step procedure is (i) protection of the 5′-OH position of thymidine with *t*-butyldimethylsilyl chloride (*34*); (ii) protection (acid labile) of the 3′-OH position with dimethoxytrityl (DMT) chloride (*35*); (iii) desilylation of the 5′ position by treatment with 1*M* tetrabutylammonium fluoride in tetrahydrofuran (*34*); and (iv) phosphitylation of the 5′ position with chloro(2-cyanoethyl)-*N*,*N*-diisopropylamino phosphite (*36*). The intermediates were purified by silica gel chromatography and the final product **4**, [5′-(2-cyanoethyl-*N*,*N*-diisopropylamino)phosphinyl-3′-dimethoxytritylthymidine], was obtained in 80 percent overall yield.

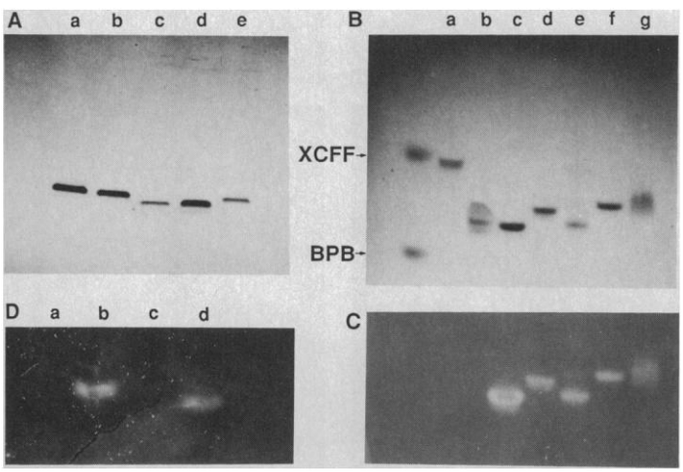

Fig. 2. Polyacrylamide gel electrophoretic analysis of ps and aps hairpins. (**A**) Denaturing 15 percent polyacrylamide gel (8*M* urea, 90 m*M* tris-borate, 5 m*M* Na-EDTA, *p*H 8.3; 60°C). (Lane a) psG; (lane b) apsG; (lane c) psC; (lane d) apsC; (lane e) $d(T)_{24}$. Visualization by ultraviolet shadowing. (**B**) Nondenaturing (10 m*M* $MgCl_2$, 90 m*M* tris-borate, *p*H 8.3) 15 percent polyacrylamide gel run at 4°C. (Lane a) $d(T)_{24}$; (lane b) $d(T)_{10}$·$d(A)_{10}$; (lane c) $d(C·G)_5$·$d(C·G)_5$; (lane d) apsC; (lane e) psC; (lane f) apsG; (lane g) psG. Visualization by ultraviolet shadowing. (**C**) Gel from (B) stained with ethidium bromide (0.5 μg ml^{-1}) at 4°C. Visualization by fluorescence. (**D**) Nondenaturing [buffer as (B)] 15 percent polyacrylamide gel run at 4°C and stained with BBI-258 (0.1 μg ml^{-1}). (Lane a) psG; (lane b) apsG; (lane c) psC; (lane d) apsC. Visualization by fluorescence.

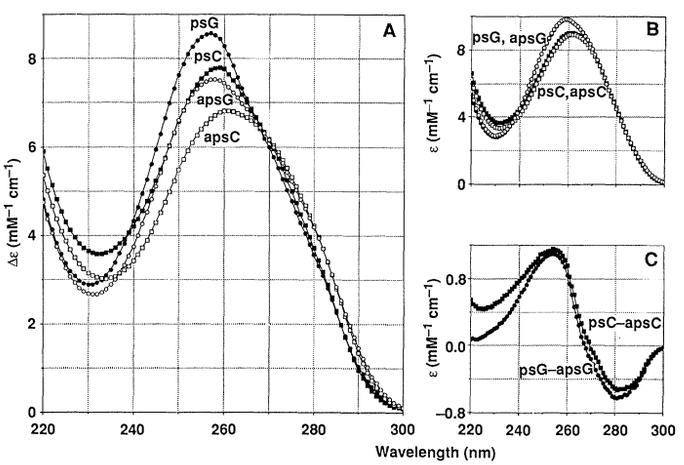

Fig. 3. Ultraviolet absorption spectra of ps and aps hairpins. (**A**) Spectra of base-paired hairpins. Conditions: 20°C, 0.1*M* NaCl, 10 m*M* sodium cacodylate, *p*H 7.2. The following wavelength (λ) and molar extinction coefficient (ε) values are in units of nm and mM^{-1} cm^{-1}, respectively. For psC: λ_{max}, 259; ε_{max}, 7.8: ε_{260} 7.8. For psG: λ_{max}, 257; ε_{max}, 8.6; ε_{260}, 8.3. For apsC: λ_{max}, 261; ε_{max}, 6.8; ε_{260}, 6.8. For apsG: λ_{max}, 258; ε_{max}, 7.5; ε_{260}, 7.4. The extinction coefficients were calculated from the observed hyperchromicities and the values for the denatured state estimated below. (**B**) Spectra of denatured hairpins. Conditions: 80°C, 0.1*M* NaCl, 10 m*M* sodium cacodylate, *p*H 7.2. For psC: λ_{max}, 261; ε_{max}, 9.0. ε_{260}, 9.0. For psG: λ_{max}, 259; ε_{max}, 9.8; ε_{260}, 9.8. For apsC: λ_{max}, 261; ε_{max}, 8.9; ε_{260}, 8.9. For apsG: λ_{max}, 259; ε_{max}, 9.8; ε_{260}, 9.8. The extinction coefficients were estimated as follows (*19*). The molar extinction coefficients of melted poly[d(C)] and poly[d(G)] are essentially the same at 275 nm (*19*). From the appropriate linear combination of extinction coefficients for denatured poly[d(A)]·poly[d(T)] (*37*) and poly[d(G)]·poly[d(C)] at 275 nm, we calculated the theoretical universal molar extinction coefficient ε_{275} = 6.4 mM^{-1} cm^{-1}. All the spectra were scaled accordingly. (**C**) Indicated difference spectra under native conditions. Δε is the difference molar extinction coefficient.

versus dG_4, are the same for both the ps and aps hairpins. This conclusion is based on the finding that the difference spectra (ps − aps) for the two sets of molecules are very similar, with the following characteristic, common features (Fig. 3C): a positive peak in the region 235 to 265 nm ($\Delta\epsilon_{255}$, +1.1 mM^{-1} cm^{-1}); a negative peak from 270 to 296 nm ($\Delta\epsilon_{281}$, −0.6 mM^{-1} cm^{-1}); and an isosbestic point at 267 nm. The blue-shifted ultraviolet absorption of the ps hairpins (compared to that of the aps counterparts) is novel for duplex DNA and indicative of changes in the electronic structures and stacking geometries of the bases in their respective helices (see below). The ultraviolet spectra under denaturing conditions (80°C) are virtually identical for the two sets of aps and ps hairpins, and provide the means for establishing the molar extinction coefficients (Fig. 3, A and B). The unusual 3′-p-3′ and 5′-p-5′ phosphodiester bonds in the ps hairpins have no perceptible effect on the ultraviolet absorption of these oligonucleotides in the random coil state. That is, the differences due to the dC_4 and dG_4 loops are consistent with the spectra reported previously for the denatured states of poly[d(C)] and poly [d(G)] (*19*).

The aps and ps hairpins were also analyzed by circular dichroism (CD) spectroscopy (Fig. 4). A comparison of the spectra of the set of ps and aps hairpins with dC loops (Fig. 4A) and dG loops (Fig. 4B) indicates that the ps hairpins have a slightly higher dichroism at the positive maximum near 220 nm but lower magnitudes at the peaks at longer wavelengths. The zero crossover points at 209 and 235 nm are the same for all hairpins, but the one near 260 nm is shifted about 5 nm to the red in the case of the ps oligomers. Thus, the difference CD spectra (ps − aps) (Fig. 4D) show striking similarities (positive peaks: 220, 245 nm; negative peaks: 255, 285 nm). These features would appear to be related to the blue shift in the ultraviolet absorption spectra of the ps oligomers. The spectra under denaturing conditions (80°C) are nearly identical for the sets of hairpins with either dC or dG loops (Fig. 4C), as was noted above in the case of the ultraviolet absorption. The overall similarity between the CD spectra of the aps and ps oligonucleotides in the native state confirms the double helical nature of the ps hairpins in particular. However, the consistent differences between the two sets of spectra are further evidence for fundamental structural distinctions. Another of the major DNA conformations, left-handed Z-DNA, is characterized by an absorption spectrum *red* shifted relative

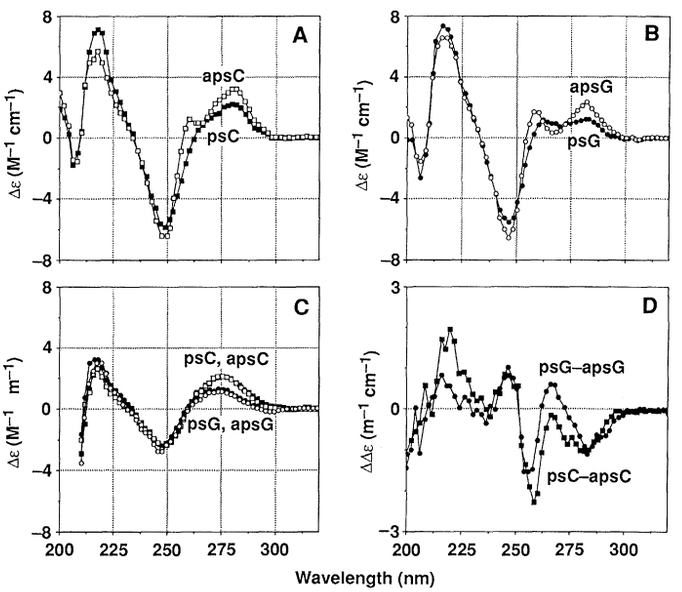

Fig. 4. Circular dichroism spectra of ps and aps hairpins. Buffer: 0.1*M* NaCl, 0.05*M* sodium phosphate, 0.1 m*M* EDTA, *p*H 7.6. (**A**) psC and apsC at 23°C. (**B**) psG and apsG at 23°C. (**C**) Spectra at 85°C of samples from (A) and (B). (**D**) Indicated difference spectra at 23°C. Δε is the difference in the molar extinction coefficient for right and left polarized light. ΔΔε is the difference between the Δε values for the indicated structures.

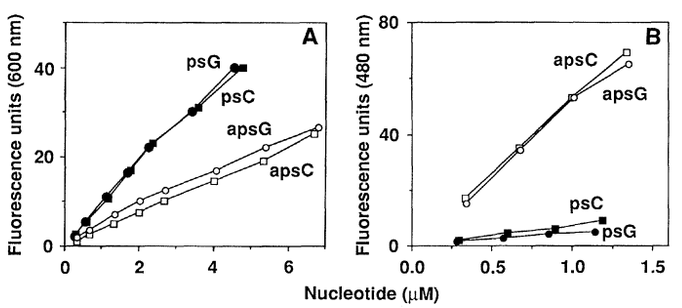

Fig. 5. Drug binding to ps and aps hairpins. Fluorescence measurements made in 0.1*M* NaCl, 0.01*M* tris-HCl, 0.1 m*M* EDTA, *p*H 8.0. (**A**) 1.3 μ*M* ethidium bromide (λ_{ex} 525 nm, λ_{em} 600 nm) and (**B**) 0.6 μ*M* BBI-258 (λ_{ex} 355 nm, λ_{em} 480 nm).

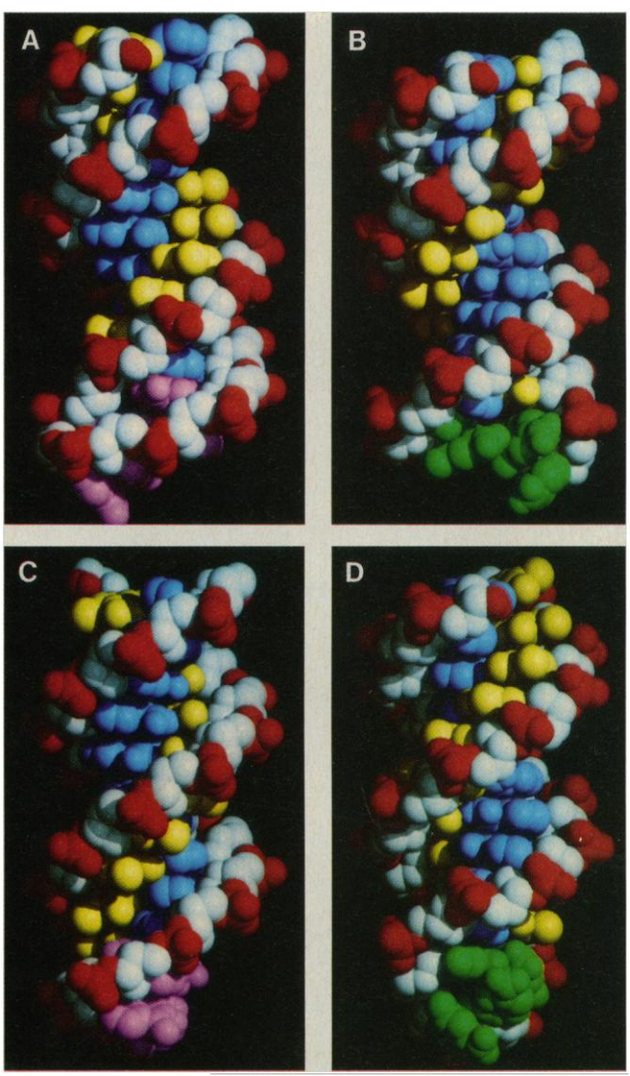

Fig. 6. Space filling models of the optimized structures of both the aps and ps hairpins showing differences in helical and loop conformations (*38*). (**A**) apsC; (**B**) apsG; (**C**) psC; (**D**) psG. (DNA backbone, white; phosphate groups, red; bases: adenine, blue; thymine, yellow; cytosine, magenta; guanine, green.)

to that of B-DNA (*20*).

Drug-DNA interactions. Upon titration of ethidum bromide with the four hairpins (Fig. 5A), the ps oligomers unexpectedly elicit nearly twice the fluorescence enhancement observed with the corresponding aps molecules. The excitation and emission spectra and the fluorescence lifetimes of the drug bound to the ps hairpins are not distinguishable from those of the control DNA (aps)–drug complexes (*21*). Thus, we conclude that binding (intercalation) of ethidium is actually facilitated in the ps compared to the aps duplexes.

The interactions of BBI-258 with the aps and ps hairpins were examined. Solution studies (*22*) and the diffraction analysis of drug-deoxyoligonucleotide co-crystals (*23*) indicate that the minor groove determinants of three to five A·T base pairs are required for specific

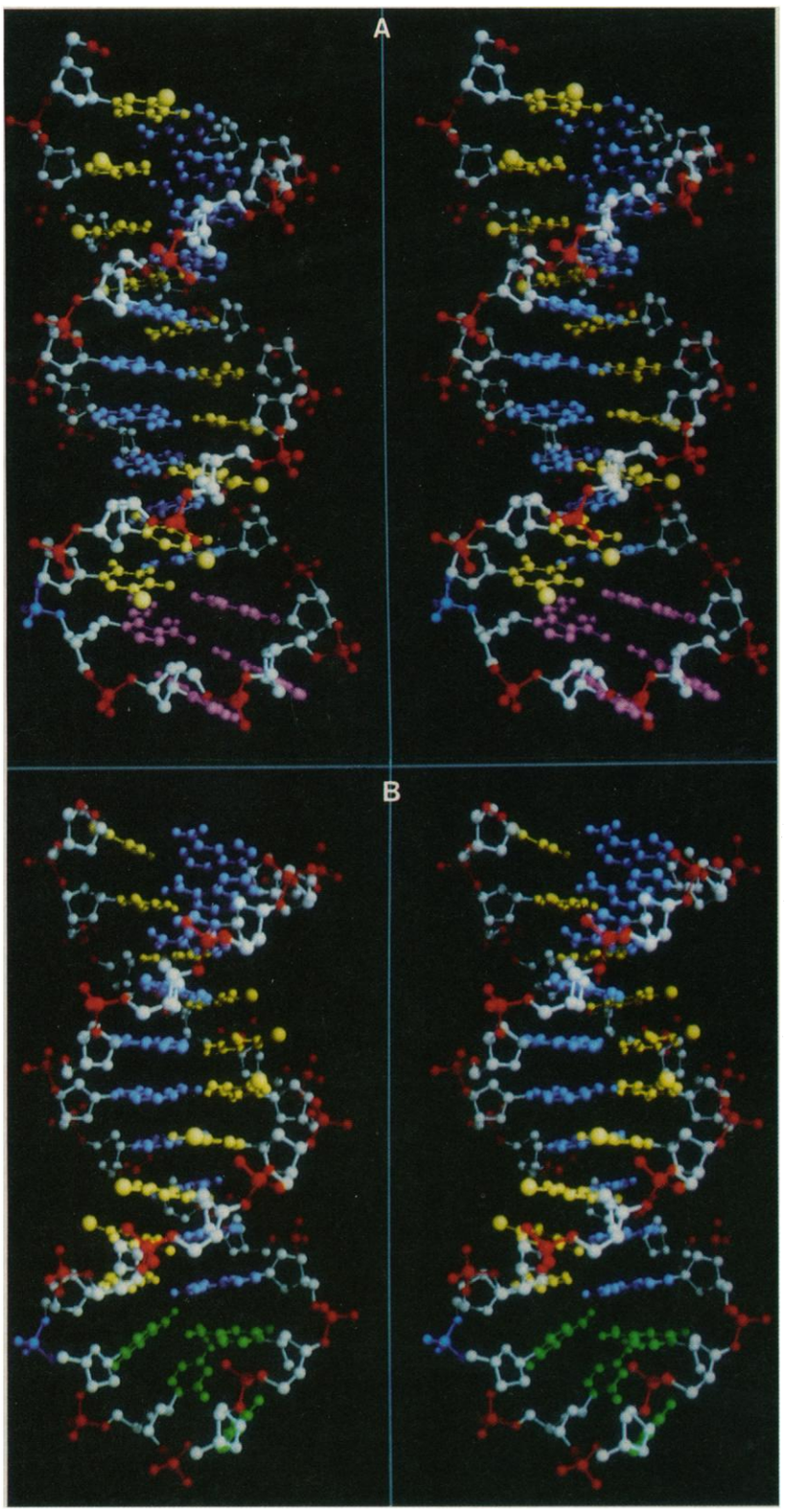

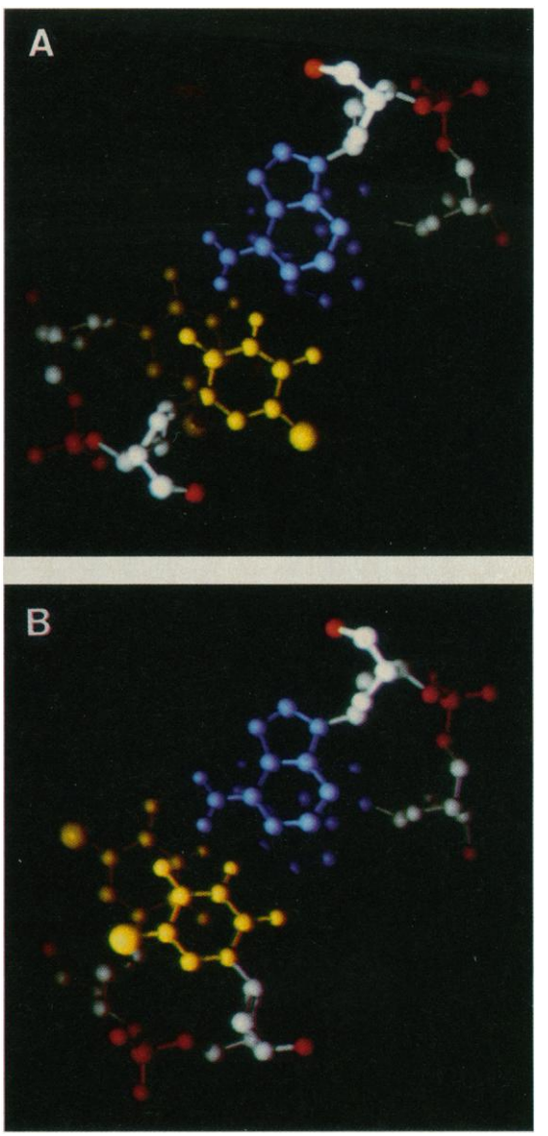

Fig. 7 (**left**). Stereo pairs of the optimized ps hairpins. (**A**) psC with the 5′-p-5′ internucleotide bond shown in dark blue. (**B**) psG with the 3′-p-3′ internucleotide bond shown in dark blue. Colors as in Fig. 6. **Fig. 8** (**right**). Base-pairing and base-stacking in the optimized ps (**A**) and aps (**B**) structures. The C5-methyl group of the thymine base is enlarged for emphasis. Colors as in Fig. 6.

binding. The drug BBI-258 induces a widening of the minor groove and a bending of the helix axis, and makes major hydrogen bonding contacts with N3 of A and O2 of T (*23*). The characteristic strong fluorescence enhancement arising from interaction with A·T-rich B-DNA (*22*) is also observed in the complexes formed by BBI-258 with the aps hairpins (Fig. 5B). In contrast, only a very small increase in fluorescence is seen in the presence of the ps oligomers. Competition experiments involving the titration of preformed drug-poly[d(A-T)] complexes with the ps hairpins indicate that the latter have a greatly reduced affinity for the drug. These findings suggest that the helical parameters of the parallel stranded duplexes are significantly different from those of conventional B-DNA, such that the presentation of hydrogen-bonding donor-acceptor functions, van der Waals contacts, specific hydration, or other stereochemical features of the ps helix (for example, the position of the C5 methyl group) are incompatible with the binding of BBI-258. Both intercalation and minor groove binding to the homopolymer duplex poly[d(A)]·poly[d(T)] are entropically driven (*24*). This observation and the appearance of novel bifurcated hydrogen-bonding patterns in crystals of oligonucleotides containing the same homopolymeric sequences (*25*) emphasize the central role of hydration patterns and groove geometry in mediating the interaction of ligands with DNA.

Base-pairing in ps DNA by chemical probing. The A·T base pair used by Pattabiraman in the energy minimization calculations of ps DNA (*12*) is the reverse Watson-Crick type, in which the thymine is rotated 180° around the N3–C6 axis from the normal Watson-Crick base pair such that the glycosyl bonds are in a trans configuration, as shown in the following diagram and in Fig. 8.

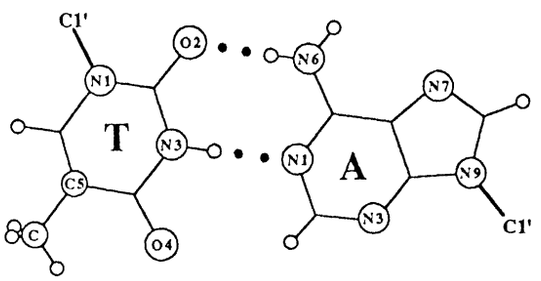

In contrast, the documented base pairing in the parallel strand of poly[d(A)]·2 poly[d(T)] is of the Hoogsteen type with the T residue interacting with the N7–C6–NH_2 face of the adenine residue (*2*). To obtain evidence in support of reverse Watson-Crick base pairing in the ps duplex structures, alkylation with [^{3}H]dimethyl sulfate was used as a probe for the available reactive sites on the base pairs of the ps and aps hairpins. The hairpins were methylated and subsequently degraded to bases, and the modified bases were separated by ion exchange chromatography (*26*). The methylated base ratios for the apsG hairpin were 19 ± 2 (*27*) for m^7G to m^3A, and 150 ± 10 for m^7G to m^1A; the corresponding values for psG methylation were 20 ± 2 and 125 ± 10, respectively. The similarity in the methylation of the aps and ps hairpins indicates that identical reactive sites on the base pairs are available for the alkylation reactions. These observations are compatible with a reverse Watson-Crick base pairing in the parallel stranded duplexes. If a Hoogsteen or a reverse-Hoogsteen base-pairing scheme had been present in these structures, the N1 of adenine would have been available for methylation, resulting in a greatly decreased ratio of m^7G to m^1A, a prediction contrary to the experimental findings.

Model structures of ps and aps hairpins from molecular mechanics calculations. In the construction of the models for the different parallel and antiparallel hairpins (*28*), a modified version of the basic AMBER software package (*29*) was used. We restrict ourselves here to general results and representative figures.

1) To construct a model for the parallel stranded helix, we used a somewhat different method from that of Pattabiraman (*12*). In a dodecamer $d(A)_{12}$·$d(T)_{12}$ constructed from Arnott's idealized B-DNA (*30*), every thymidylate residue (base, sugar, and phosphate group) was rotated such that the C6, O2, and O4 atoms of the base were mapped on to the positions of the corresponding C6, O4, and O2 atoms in the original B-DNA, thereby establishing the reverse Watson-Crick base pair. The model parallel double-helical structure was optimized with the imposition of helical symmetry constraints (*31*) on all but the terminal base pairs, a procedure that prevents the structure from losing the helical symmetry of the starting coordinates in the first stage of optimization. In the last step of minimization, all constraints were omitted. The resulting energies are comparable to those of Pattabiraman's, that is, they show that the aps helix [corresponding to entry B_1 in (*31*), table 1] is somewhat favored over the ps helix, in agreement with the T_m measurements.

2) To construct the hairpins, we generated the different four-base loops for the oligomers containing dG's and dC's graphically with the use of the Insight package (Biosym Technologies) on an Evans & Sutherland PS350 (PS390) molecular graphics work station, and connected them to decameric helices of both the ps and aps DNA's described above. Special care was exercised in optimizing the stacking of the bases in the loop (pur-pur favored over pur-pyr). A first minimization was carried out on the initial coordinates with the use of harmonic constraints to relax bad contacts. The structures were then further optimized by allowing the four bases in the loop to reorientate, thereby generating starting structures for the last stage of calculation, resulting in Figs. 6 and 7. The ps helix (Fig. 6, C and D, and Fig. 7), as opposed to the aps B-DNA structures (Fig. 6, A and B), lacks a clear distinction between a major and a minor groove. This rough equivalence of the grooves leads to more compact loops in the ps hairpins. A distinctive feature of the aps structures is the extension of the minor groove into the loop. Both the ps and aps helices have a C2′ endo sugar puckering in both strands and a helical twist of about 42°. The rise per base pair and propeller twist are ~3.2 Å and ~20° in the ps helix; the corresponding values for the aps helix are ~3.0 Å and 22°. Because of the symmetry in the thymine base, the hydrogen bonds between the A·T base pairs in the resulting parallel helix are of the same type as in the antiparallel structure. However, the C5 methyl group is now directed into what is formally the minor groove of the ps helix, and the pyr-pyr stacking and to a lesser degree the pur-pur stacking are necessarily different (Fig. 8).

Obviously, the reliability of the calculated models could be further improved by including structural information from other experiments, such as bounds on proton-proton distances gained from nuclear magnetic resonance (NMR) measurements. Initial ^{1}H-NMR spectra of hairpins similar to those described above provide indication of distinct differences between the ps and aps conformations, but a detailed 2-D NMR analysis is not yet available.

Generalizations of the ps structure. Our experimental results and the molecular graphics calculations provide evidence that DNA containing A·T base pairs can form a stable parallel stranded duplex structure, designated here as ps-DNA (*32*). We anticipate that the molecular details of ps-DNA will be provided by crystallographic and more extensive spectroscopic analysis. The compositional requirements for ps-DNA need to be established. The hydrogen bonding potential of a reverse Watson-Crick A·T base pair is essentially that of the conventional Watson-Crick structure. In DNA with sequences containing G·C, the adoption of the ps conformation would lead to a loss of at least one hydrogen bond per reverse Watson-Crick G·C base pair (*2, 33*), unless compensating tautomerizations were to occur. Does this consideration imply that parallel stranded DNA structures are limited to A·T containing DNA?

Additional questions relate to the topological implications, to the compatibility with RNA and DNA-RNA hybrids, and, of course, to the possible biological functions of ps-DNA. The finding that A·T containing DNA can exist in an alternative rather stable parallel stranded conformation provides yet another major duplex conformation to consider in the assignment of polynucleotide structures and serves to emphasize further the structural diversity of DNA.

REFERENCES AND NOTES

1. S. Arnott, *Prog. Biophys. Mol. Biol.* **21**, 267 (1970); R. E. Dickerson *et al.*, *Science* **216**, 475 (1982).
2. W. Saenger, *Principles of Nucleic Acid Structure* (Springer-Verlag, New York, 1984).
3. R. E. Dickerson, in *Unusual DNA Structures*, R. D. Wells and S. C. Harvey, Eds. (Springer-Verlag, New York, 1988), pp. 287–306.
4. E. Westhof and M. Sundaralingam, *Proc. Natl. Acad. Sci. U.S.A.* **77**, 1852 (1980).
5. M. H. Sarma, G. Gupta, R. H. Sarma, *FEBS Lett.* **205**, 223 (1986).
6. A. Rich, D. R. Davies, F. H. Crick, J. D. Watson, *J. Mol. Biol.* **3**, 71 (1961).
7. F. Ishikawa, J. Frazier, F. B. Howard, H. T. Miles, *ibid.* **70**, 475 (1972); T. Hakoshima, T. Fukui, M. Ikehara, K.-I. Tomita, *Proc. Natl. Acad. Sci. U.S.A.* **78**, 7309 (1981).
8. J. S. Lee, D. A. Johnson, A. R. Morgan, *Nucleic Acids Res.* **6**, 3073 (1979); J. S. Lee, M. L. Woodsworth, L. J. P. Latimer, A. R. Morgan, *ibid.* **12**, 6603 (1984); D. E. Pulleyblank, D. B. Haniford, A. R. Morgan, *Cell* **42**, 271 (1985); S. M. Mirkin *et al.*, *Nature* **330**, 495 (1987). Abbreviations: pyr, pyrimidine; pur, purine.
9. H. E. Moser and P. B. Dervan, *Science* **238**, 645 (1987).
10. L. H. Koole, M. H. P. van Genderen, H. M. Buck, *J. Am. Chem. Soc.* **109**, 3916 (1987).
11. F. Morvan *et al.*, *Nucleic Acids Res.* **15**, 7027 (1987); N. T. Thuong, U. Asseline, V. Roig, M. Takasugi, C. Hélène, *Proc. Natl. Acad. Sci. U.S.A.* **84**, 5129 (1987); D. Praseuth *et al.*, *J. Mol. Biol.* **16**, 939 (1987).
12. N. Pattabiraman, *Biopolymers* **25**, 1603 (1986).
13. M. D. Matteucci and M. H. Caruthers, *Tetrahedron Lett.* **21**, 719 (1980).
14. M. W. Germann, R. T. Pon, J. H. van de Sande, *Anal. Biochem.* **165**, 399 (1987).
15. G. Chaconas and J. H. van de Sande, *Methods Enzymol.* **65**, 75 (1980).
16. N. B. Ramsing and T. M. Jovin, in preparation.
17. K. J. Breslauer, R. Frank, H. Blöcker, L. A. Marky, *Proc. Natl. Acad. Sci. U.S.A.* **83**, 3746 (1986).
18. D. Erie, N. Sinha, W. Olson, R. Jones, K. Breslauer, *Biochemistry* **26**, 7150 (1987).
19. R. B. Inman, *J. Mol. Biol.* **9**, 624 (1964); C. F. Lefler and F. J. Bollum, *J. Biol. Chem.* **244**, 594 (1969).
20. T. M. Jovin, D. M. Soumpasis, L. P. McIntosh, *Annu. Rev. Phys. Chem.* **38**, 521 (1987).
21. G. Marriott, N. B. Ramsing, R. C. Clegg, T. M. Jovin, unpublished data.
22. S. A. Latt and G. Stetten, *J. Histochem. Cytochem.* **24**, 24 (1976); T. Stokke and H. B. Steen, *ibid.* **33**, 333 (1985); K. D. Harshman and P. B. Dervan, *Nucleic Acids Res.* **13**, 4825 (1985); K. F. Jorgensen, V. Varsheny, J. H. van de Sande, *J. Biomol. Struct. Dyn.* **5**, 1005 (1988).
23. P. E. Pjura, K. Grzeskowiak, R. E. Dickerson, *J. Mol. Biol.* **197**, 257 (1987).
24. K. J. Breslauer *et al.*, *Proc. Natl. Acad. Sci. U.S.A.* **84**, 8922 (1987).
25. H. C. M. Nelson, J. T. Finch, B. F. Luisi, A. Klug, *Nature* **330**, 221 (1987); M. Coll, C. A. Frederick, A. H.-J. Wang, A. Rich, *Proc. Natl. Acad. Sci. U.S.A.* **84**, 8385 (1987).
26. A. D. Mirzabekov and A. F. Melnikova, *Mol. Biol. Rep.* **1**, 379 (1974).
27. The given range indicates the limits of experimental values.
28. W. Elhorst, E. v. Kitzing, T. M. Jovin, in preparation.
29. P. K. Weiner and P. A. Kollman, *J. Comput. Chem.* **2**, 287 (1981).
30. S. Arnott and D. W. L. Hukins, *Biochem. Biophys. Res. Commun.* **47**, 1504 (1972).
31. E. v. Kitzing and S. Diekmann, *Eur. Biophys. J.* **15**, 13 (1987).
32. In the course of review we were queried about a possible alternative structure for the psC and psG oligomers consisting of an antiparallel duplex (eight to ten nucleotides long) with ends bridged by a single-stranded segment containing the dG_4 or dC_4 sequences. We exclude this possibility for the following reasons. (i) Stereochemical considerations would limit the maximal duplex length to seven or eight nucleotides; the accompanying loss of thermodynamic stability would probably be incompatible with the values of Table 1 and with the very similar properties of related hairpins we have studied containing only eight nucleotides in the stem region. In addition, the loop in the alternative structure would necessarily interact with the duplex segment, possibly accounting for the observed spectral pertubations except for the fact that they are the same for psC and psG. (ii) Ethidium bromide intercalation would be expected to severely strain or disrupt the proposed structure, yet the drug binds even better to the ps than to the aps oligomers. (iii) The reactions with polynucleotide ligase are compatible with the existence of only one end in the monomeric oligomers. (iv) Very similar properties are observed with ps-DNA in the form of duplexes formed from linear oligonucleotides with appropriate sequences (N. B. Ramsing and T. M. Jovin, *Nucleic Acids Res.*, in press; M. W. Germann, B. W. Kalisch, J. H. van de Sande, in preparation).
33. A reverse G·C Watson-Crick base pair has been observed in crystals of yeast phenylalanine transfer RNA ($tRNA^{Phe}$) [S.-H. Kim, *Prog. Nucl. Acid Res. Mol. Biol.* **17**, 181 (1976); A. Klug, J. Ladner, J. D. Robertus, *J. Mol. Biol.* **89**, 511 (1974)], but it is not isomorphous with the reverse A·T base-pair in the DNA structures we have discussed.
34. K. K. Ogilvie, *Can. J. Chem.* **51**, 3799 (1973).
35. M. Smith, D. H. Rammler, I. H. Goldberg, H. G. Khorana, *J. Am. Chem. Soc.* **84**, 430 (1962).
36. N. D. Sinha, J. Biernat, J. McManus, H. Koster, *Nucleic Acids Res.* **12**, 4539 (1984).
37. M. Riley, B. Maling, M. J. Chamberlin, *J. Mol. Biol.* **20**, 359 (1966); R. B. Inman and R. L. Baldwin, *ibid.* **8**, 452 (1964).
38. The molecular graphics program SCHAKAL (version 86b) of Dr. E. Keller, University of Freiburg, was used in the generation of this figure and the other model structures.

39. Supported in part by the Medical Research Council of Canada and the Alberta Heritage Foundation for Medical Research.

22 February 1988; accepted 31 May 1988.